ELSEVIER

Biophysical Chemistry 53 (1994) 105–114

Biophysical Chemistry

How random is a highly denatured protein?

P. Calmettes [a,*], D. Durand [a], M. Desmadril [b], P. Minard [b], V. Receveur [a], J.C. Smith [c]

[a] *Laboratoire Léon Brillouin (CEA-CNRS), CE-Saclay, 91191 Gif-sur-Yvette Cedex, France*

[b] *Laboratoire d'Enzymologie Physico-chimique et Moléculaire, Groupe de Recherche du CNRS, Université de Paris-Sud, 91405 Orsay Cedex, France*

[c] *Département de Biologie Cellulaire et Moléculaire, CE-Saclay, 91191 Gif-sur-Yvette Cedex, France*

Received 10 November 1993; revised 29 April 1994; accepted 2 May 1994

Abstract

There has been renewed interest in determining the physicochemical properties of denatured states of proteins. In many denatured states there is evidence for the existence of nonrandom configurational distributions. Here we examine the small-angle neutron scattering profile of yeast phosphoglycerate kinase in the native state and in highly denaturing conditions. We show that the denatured protein scattering profile can be interpreted using a model developed for synthetic polymers in which the chain behaves as a random coil in a good solvent, i.e. with excluded volume interactions. The implications of this result for our appreciation of the protein folding process are discussed.

Keywords: Denatured protein; Phosphoglycerate kinase; Small-angle neutron scattering; Polymer theory

1. Introduction

Globular proteins fold into specific, functional three-dimensional structures that are determined by their amino acid sequences [1]. In vitro, highly unfolded proteins can sometimes reversibly refold into the native state [2] and there is evidence that the folding pathways concerned may be similar to those occurring in cells [2,3]. Thus, in vitro experiments can provide information on the physicochemical factors determining the kinetics and thermodynamics of protein folding in vivo [4–7].

Protein folding proceeds from a 'highly' or 'completely' denatured state through partially folded intermediates to the native state. Therefore, a determination of the configurational distribution of the highly denatured state is a prerequisite for a complete understanding of protein folding pathways. Further interest in the characterization of denatured states has arisen as these states appear to be the forms recognized by chaperones, by protein complexes that initiate transport across biological membranes and by proteases responsible for intracellular protein turnover [8].

Although for most proteins the physiological denatured states are too unstable to be studied, proteins can be denatured in several ways using, for example, heat, acid or solvents. The properties of the denatured states thus obtained have been found to depend critically on the denaturing conditions [4]. Under mild denaturing conditions a globular protein may adopt a compact non-native form with a significant amount of residual structure [9]. Further denaturing may lead to an expansion of the structure with a further loss of local interactions [10].

The stability of a protein towards reversible denaturation is determined by the free energy difference

* Corresponding author.

SSDI 0301-4622(94)00081-T

between the native and denatured states under the conditions of study. The free energy of a state depends on the configurations and interactions present in it. Detailed atomic-resolution information on the native structures of proteins can be obtained using NMR spectroscopy or X-ray crystallography. However, structural information on highly denatured states is much less accessible as their conformational flexibility prevents their crystallisation and reduces the information obtainable using multidimensional NMR spectra. Therefore, until quite recently, most biophysical research aimed at understanding the principles of protein stability relied exclusively on examinations of the native state, and this is still the preferred approach in some laboratories [11]. However, changes in the interactions present in the denatured state can, in principle, affect the stability of a protein. Changes in the free energy of the denatured state upon, for example, site-directed mutagenesis, will influence the relative stabilities of the native forms. Indeed, evidence that the denatured form can play a significant role in stability differences has been provided by experiments on staphylococcal nuclease [12]. A significant fraction of the stability loss accompanying point mutations in this protein was attributed to changes in solvent exposure in the denatured state.

Recently, much progress has been made in finding out information about the structures of denatured proteins and in trapping and characterising kinetic folding intermediates. NMR, in particular, has provided a major impetus in this regard. A combination of pulsed hydrogen exchange experiments with NMR has allowed the detailed characterization of interactions present in denatured states of some small proteins that may correspond to intermediates along their folding pathways [13,14].

Most of the present, widely used techniques for the investigation of denatured states, such as NMR and the various optical spectroscopies, probe protein conformation on relatively short length scales. To complement these approaches small-angle scattering (SAS) using either neutrons (SANS) or X-rays (SAXS) can provide information on low resolution global structural features of denatured proteins [15–20]. SAS experiments have recently started to be applied to the characterization of denatured states. For instance, SAXS has been used to examine the salt-mediated conversion of the moderately expanded acid-denatured form of cytochrome c to a compact molten globule form [18]. Heat-denatured states have also been examined by small-angle scattering. Using SAXS it was found that thermally denatured ribonuclease A undergoes only a 30% increase in its radius of gyration when its disulphide bonds are intact [19]. Upon reduction of these bonds the heat-denatured and 6 M guanidinium chloride-denatured forms increased greatly in size, yet remaining much smaller than predicted for a random coil. SAXS has been applied to the examination of the staphylococcal nuclease mutants mentioned above [17]. The results showed that single amino acid substitutions can radically alter the configurational distribution of a partially condensed polypeptide chain.

In the present paper we will be concerned with a highly denatured protein. A highly denatured protein can be produced, without disrupting the covalent structure of the polypeptide chain, with high concentrations of urea or guanidinium chloride (Gdn-HCl). As a first approximation for experiments on protein folding, this state has been considered as 'fully unfolded', that is as a random coil with conformations limited only by steric interactions between the atoms. More recently, however, it has become apparent that some highly denatured proteins can still possess significant residual structure. For example, NMR studies of 434-repressor in 7 M urea have provided evidence that a cluster of hydrophobic residues exists [21]. Results such as these call into question the idea that even highly denatured proteins behave as random polymers.

In a recent paper [16] we applied the SANS technique to obtain information on the configurational distribution of highly denatured yeast phosphoglycerate kinase (PGK), an enzyme involved in the first step of glycolysis. PGK is a two-domain monomeric globular protein of 44525 Da consisting of 415 amino acids and no disulphide bridges [22]. Its folding pathway has been widely studied using spectroscopic and biochemical methods [23]. In a previous work [16] the SANS data showed that the denaturation was accompanied by a large increase in the radius of gyration of the protein. The data were further interpreted using statistical mechanical and molecular mechanical modelling procedures to obtain a description of the configurational distribution of the denatured chain. In the statistical mechanical model the region of contrast scattering density associated with the protein chain was pictured as a chain of freely-jointed spheres. It was found that a

model with a small number of spheres could not fit the data; a good fit was obtained with 100 spheres of 8.5 Å radius. Single configurations of the fitted chain of spheres were used as low-resolution bounds for model-building and molecular mechanics calculations to obtain plausible atomic models of individual denatured chain configurations.

An alternative and complementary approach to interpreting the SANS data involves the use of analytical polymer theories to describe the chain configurational distribution. In this article we present improved experimental SANS scattering profiles and describe them using theoretical expressions commonly used for synthetic homopolymers [24,25]. The results allow a better determination of the radius of gyration of the denatured molecule and enable distinctions to be made between different polymer models that might be applicable to the description of the protein chain.

In Section 2, the experimental procedures are briefly described. In Section 3, SANS profiles are presented for native and denatured PGK. Polymer models are fitted to the results obtained for the denatured form. We find that the data can be described by a model in which the chain behaves as a random coil with excluded volume interactions.

2. Materials and Methods

The experiments were performed in heavy water (D_2O) with deuterated guanidinium chloride (Gdn-DCl). This choice has three main advantages: (i) The scattered intensity is higher than in H_2O; (ii) incoherent scattering is reduced to a minimum; (iii) Gdn-DCl has a scattering power density almost identical to that of D_2O so that excess coherent scattering arises mainly from the solute polypeptide.

2.1. Materials

Yeast phosphoglycerate kinase and deuterated guanidinium chloride were prepared and purified as follows.

2.1.1. Yeast phosphoglycerate kinase

Just before the scattering experiments, recombinant PGK was prepared as described previously [26]. The purified protein was transferred to 50 mM deuterated Tris buffer, pD 7.2, by desalting on a G25 Sephadex column. The enzyme activity was checked as described in ref. [27] using a coupled assay with glyceraldehyde-3-phosphate dehydrogenase. The protein concentration in the stock solution was determined by both BCA protein assay [28] and light absorbance at 279 nm, using $\epsilon = 0.49$ ml/mg cm.

2.1.2. Deuterated guanidinium chloride

Sequanal grade Gdn-HCl was purchased from Pierce (Rockford, IL, USA, catalogue No. 24110) and 99.8% enriched D_2O from Eurisotop (Saint-Aubin, France, catalogue No. D214H). These chemicals were used without further purification. The Gdn-HCl was dissolved in D_2O at a concentration of about 4 M. The solution was gently degassed under vacuum at room temperature and the D_2O evaporated at 40°C in a vacuum oven. This procedure was repeated four times in the same flask. Before the last evaporation the solution was filtered through 0.1 mm pore-size nylon membrane filters (Nalge Co., Rochester, NY, USA). An 8 M stock solution was prepared by dissolving the dry salt in a suitable amount of D_2O. The solution pD was adjusted to the same value as that of the buffer and the final denaturant concentration was measured by refractometry.

Samples for neutron scattering experiments were prepared in a cold room at 8°C by mixing suitable volumes of the protein and the denaturant stock solutions with the deuterated buffer. Control samples of solvent alone were simultaneously prepared using the same pipette settings. Scattering profiles of the native and denatured protein were measured at 14.8 ± 0.2°C with a protein concentration of 5 mg/ml.

2.2. Neutron scattering

In this article we present experimental SANS profiles that are improved compared to the previously published results [16]. A careful reexamination of the previous profiles indicated that there may have been a slight aggregation of the denatured PGK molecules due to insufficient temperature stability during sample preparation. The effect of aggregation on the scattering profiles is essentially confined to the region used to determine the radius of gyration. However, the improved value for the radius of gyration obtained in the present work is still within 10% of the previous value.

The SANS measurements were carried out with the PACE instrument at the Laboratoire Léon Brillouin, C.E. Saclay, France. Scattering intensities were simultaneously recorded at different scattering angles using neutrons of wavelengths, $\lambda = 5.0$ and 11.0 Å. Different sample-to-detector distances were selected to obtain wavevector transfers, q, ranging from about 8×10^{-3} $Å^{-1}$ to about 7×10^{-1} $Å^{-1}$. The wavevector transfer is defined as

$$q = \frac{4\pi}{\lambda}\sin(\tfrac{1}{2}\theta), \qquad (1)$$

where θ is the scattering angle.

All the samples were contained in fused silica spectrophotometer cuvettes of 5.00 mm path length (Hellma, France). Scattering intensities were corrected for non-uniformity of the detector response by normalization to the mainly incoherent scattering from a 1.00 mm thick water sample whose absolute differential cross-section was measured to be 0.81 ± 0.02 cm^{-1} $sterad^{-1}$ at $\lambda = 5.0$ Å [16,29] and 0.98 ± 0.02 cm^{-1} $sterad^{-1}$ at $\lambda = 11.0$ Å.

In each case the scattering spectra of the solvent alone were subtracted from those of the solution. Each resulting spectrum was further corrected for excess incoherent scattering from the protein solution compared to the buffer. This scattering contribution arises mainly from the protein hydrogen atoms which were not exchanged in the deuterated stock solutions. In the q range investigated the level of incoherent scattering is constant. At the largest q values, the coherent scattering of the solution is negligible with respect to the incoherent contribution. Consequently, the excess incoherent scattering was subtracted in such a way that the remaining intensity almost vanishes for $q \geqslant 0.55$ $Å^{-1}$. The incoherent background subtracted in this way was very close to that computed using the hydrogen atom content of the solution and the incoherent cross-section of a bound hydrogen atom. The level of the incoherent background contribution to the spectra obtained with $\lambda = 11$ Å was assumed to be the same as for $\lambda = 5$ Å. In fact, this level might be expected to be slightly higher at $\lambda = 11$ Å than at $\lambda = 5$ Å [30]. However, this would lead to negligible systematic errors because the signal-to-noise ratio is always higher than 30 in the q range corresponding to $\lambda = 11$ Å.

3. Results and Discussion

3.1. Experimental results

3.1.1. Native PGK

The SANS profile of native PGK is shown in Fig. 1. The radius of gyration R_g was determined from the small q data using the Guinier approximation [31]

$$\ln I(q) = \ln I(0) - \tfrac{1}{3}x, \qquad (2)$$

where $x = (qR_g)^2$. Eq. (2) was fitted to the experimental data over the range 3.0×10^{-4} $Å^{-2}$ $12{,}4 \leqslant q^2 \leqslant 2.4\times10^{-3}$ $Å^{-2}$. The upper limit of this fitting range (corresponding to $x \leqslant 1.3$) is sufficiently low that the Guinier approximation is expected to be valid. The resulting value for R_g is 23.4 ± 0.2 Å. When the upper limit of the fitting range was varied between 1.3 and 0.7 the result for R_g remained constant within the stated uncertainty. As the concentration of PGK was low (5 mg/ml) the above value of R_g may be reasonably expected to be close to that at zero concentration. The result is also in fair agreement with other determinations of R_g of PGK using X-ray scattering [32,33].

3.1.2. Highly denatured PGK

The coherent SANS profile of a 5 mg/ml solution of PGK denatured in 4 M Gdn-DCl is presented in Fig. 1. The denaturant concentration is far higher than that corresponding to the midpoint (0.8 M) of the denaturation curve [23,34]. Consequently, PGK is expected

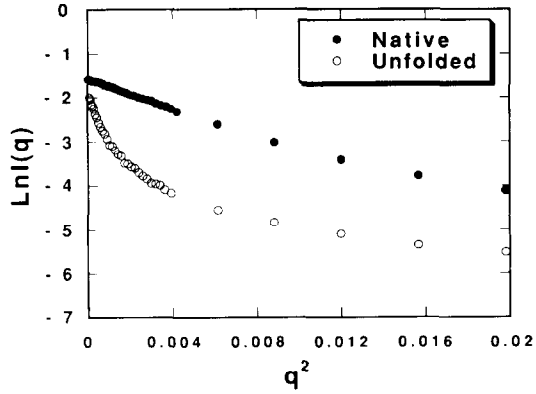

Fig. 1. Guinier plot of the SANS coherent scattering profiles of PGK in the native state (●) and denatured with 4.0 M Gdn-DCl (○): $I(q)$ is in cm^{-1} $sterad^{-1}$ (differential cross sections) and q is in $Å^{-1}$.

to be highly or fully unfolded at the denaturant concentration used. For $q \leqslant 0.25$ Å^{-1} this spectrum is very different from that of the native protein. In what follows, we interpret the scattering in terms of random polymer solution theory.

3.2. Theory of polymers in solution

Random coil theory has been widely developed to describe the behaviour of synthetic homopolymers in solution [24,25]. Because of its local stiffness a polymer can be regarded as rigid over a length b, which is called the statistical length. Consequently the polymer can be described theoretically as a chain of N freely-jointed rigid rods of length b. The contour length, L, of the chain is therefore Nb. The overall size of the polymer chain is characterized by its radius of gyration R_g.

The polymer chain can be solubilized in solvents with different physical properties. In a 'good' solvent the chain is fully solvated. Monomers far apart along the chain cannot come into close contact because of solvophilic forces. Thus, the effective interactions between the monomers are repulsive. This excludes the polymer solvation layer from the configuration space of the chain which is then said to have excluded volume. Its radius of gyration follows the scaling law

$$R_g = R_0 (L/b)^{\nu}, \tag{3}$$

where R_0 depends on both the chain stiffness and the excluded volume interactions. The exponent ν is the excluded volume exponent; its value was first calculated by Flory who found $\nu = 3/5$ [35] whereas recent field theory gives $\nu = 0.588$ [36].

In a so-called θ-solvent, the excluded volume vanishes and the chain can be equally well in contact with itself or with the solvent. In this case the probability density for distances between points on the chain is Gaussian and the chain is said to be Gaussian. It is more compact than in a good solvent. Its radius of gyration is given by Eq. (3) with $R_0 = b/\sqrt{6}$ and $\nu = 0.5$. Finally in a bad solvent the polymer chain collapses and becomes compact. Its radius of gyration is then proportional to the cube root of its contour length.

The SAS profiles of random coils have been well characterized theoretically and experimentally. To discuss this point it is convenient to introduce the normalized structure factor

$$P(q) = I(q)/I(0). \tag{4}$$

3.2.1. Low q scattering

For $0 \leqslant q \leqslant 3R_g^{-1}$ scattering experiments give information about the global size and shape of the macromolecule. Under these conditions the normalized structure factor of a random coil can be described by the Debye function [37]

$$P_D(x) = \frac{2}{x^2}(x - 1 + e^{-x}), \tag{5}$$

where $x = (qR_g)^2$. This expression is valid for Gaussian and excluded volume chains [38,39]. To within less than $\pm 0.4\%$, this function can be approximated as

$$[P_D(x)]^{-1} = 1 + 0.359x^{1.103}, \tag{6}$$

for $1 \leqslant x \leqslant 13$. A plot of the reciprocal scattering profile of denatured PGK as a function of $q^{2.206}$ is shown in Fig. 2. The Debye function fits well over the range $0 \leqslant x \leqslant 9$. The radius of gyration, calculated from the intercept and the slope of this line, is found to be 71.5 ± 2.0 Å.

This value of the radius of gyration determined using the Debye function is likely to be accurate for the following reasons. The range of validity of the commonly used Guinier approximation [Eq. (2)] is rather short for a random coil ($x \leqslant 0.3$). As few data points are collected in this range the value of R_g is uncertain. Moreover, the scattering intensities at these small q values are likely to be affected by interparticle interference, particularly if the measurements are carried out at relatively high concentrations. As a result, the apparent value of R_g is concentration dependent. Usu-

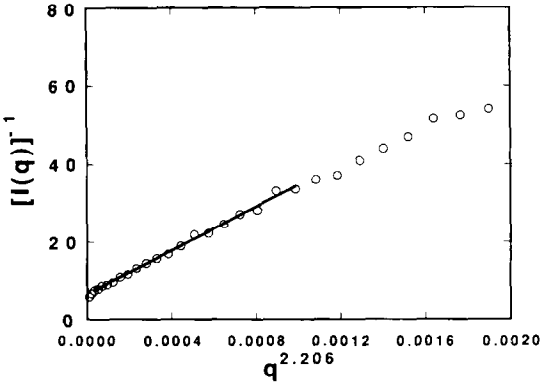

Fig. 2. Reciprocal coherent SANS profile $[I(q)]^{-1}$, as a function of $q^{2.206}$ for unfolded PGK. Using the approximation (Eq. (6)) to the Debye function (Eq. (5)) the radius of gyration of the protein is given by $R_g = (a/0.359b)^{0.453}$, where a is the slope and b the intercept of the straight line: $I(q)$ is in cm^{-1} sterad^{-1} and q in Å^{-1}.

ally one determines it at different concentrations and extrapolates to zero concentration. In the present work the value of R_g was inferred from the Debye equation using scattering data collected over a much larger q range ($1 \leqslant x \leqslant 9$) than that applicable using the Guinier approximation. In this way high q data are incorporated in the fitting range. These data are much less affected by interparticle interference than low q ones. Furthermore, in the present experiment the concentration of the scatters was rather low. Consequently we expect the value of R_g obtained here to be close to the zero concentration value.

Measurements have been performed [30] to estimate the contribution of intermolecular correlations to scattering profiles from random polymers. Using 5×10^4 Da deuterated polystyrene in a good solvent it was found that at a polymer concentration of 25 mg/ml the intermolecular interference becomes negligible for $x \geqslant 36$. Using the Zimm model [30,40] and the experimental results of ref. [30] leads to the estimation that, for the present experiments on PGK, interference effects are negligible for $x \geqslant 4$. This again suggests that the approach used here to determine R_g is quite reasonable.

3.2.2. *Intermediate q scattering*

We now consider the form of the SANS profile in the intermediate q range corresponding to $3R_g^{-1} \leqslant q \leqslant 1.4b^{-1}$. In this range the scattering probes the long-ranged internal structure of the chain. According to random polymer theory the scattering profile can be expressed as

$$P(q) = \tilde{P}_\infty x^{-1/2\nu}. \qquad (7)$$

The exponent ν is the excluded volume exponent introduced in Eq. (3). Its determination allows the distinction to be made between different polymer models, e.g. Gaussian or excluded volume chain. For a Gaussian chain $\nu = 0.5$ and the scattering intensity varies as q^{-2}. For this reason it has been common practice in SAS experiments to present data in terms of a Kratky plot, $q^2 I(q)$ versus q. In the case where the scatterers obey Gaussian statistics a Kratky plot will contain a plateau region in the intermediate q range. A Kratky plot for the native and denatured forms of PGK is presented in Fig. 3. The scattering for the native form is typical of globular proteins. For the denatured form there is no

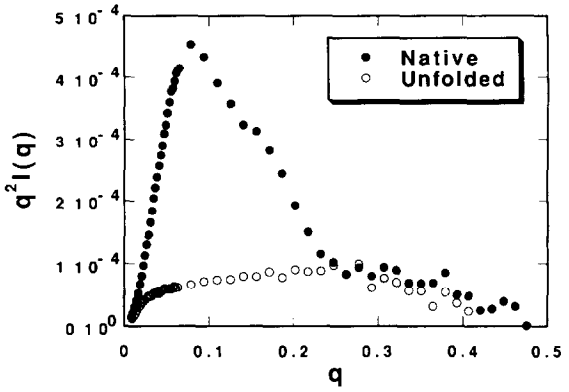

Fig. 3. Kratky plot of the SANS profiles of PGK in the native form and denatured in 4 M Gdn-DCl: $I(q)$ is in cm^{-1} $sterad^{-1}$ and q in $Å^{-1}$.

plateau at intermediate q values indicating that the polypeptide is not a Gaussian chain.

A Kratky plot cannot be conveniently used to obtain quantitative information on the configurational distribution in the intermediate q regime. To obtain this we draw a log–log plot as shown in Fig. 4. This figure indicates that in the q range corresponding to $3R_g^{-1} \leqslant q \leqslant 0.20$ $Å^{-1}$ the scattering profile of the unfolded protein can indeed be described by Eq. (7). The apparent value of the excluded volume exponent derived from the slope is $\nu = 0.58 \pm 0.02$. This is consistent with a description of the chain as a random polymer with excluded volume interactions ($\nu = 0.588$). The value $\nu = 1/2$, corresponding to a Gaussian chain, is ruled out by the data.

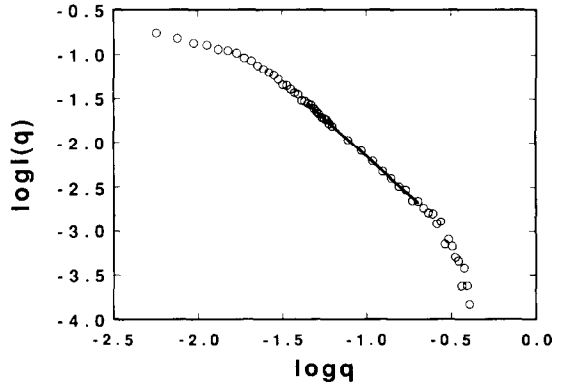

Fig. 4. Log–Log plot of the coherent neutron scattering spectrum, $I(q)$, of PGK in the denatured state in 4 M Gdn-DCl. For 4.5×10^{-2} $Å^{-1} \leqslant q \leqslant 2 \times 10^{-1}$ $Å^{-1}$ the slope $1/2\nu = -1.72$ of the straight line is, giving $\nu = 0.58$: $I(q)$ is in cm^{-1} $sterad^{-1}$ and q in $Å^{-1}$.

The prefactor $\bar{P}_\infty$ in Eq. (7) is, like ν, also a universal constant. For a Gaussian chain its value is $\bar{P}_\infty = 2$. For a chain with excluded volume the theoretical value of the prefactor is much more approximate than that of the exponent. Different models of an excluded volume chain lead to different values of $\bar{P}_\infty$ [30]. $\bar{P}_\infty$ has been calculated by means of renormalization group theory [41,42] to be ≈ 1.11. Experimental determinations have given $\bar{P}_\infty \approx 1.3$ [30,39,43]. In the present experiment the amplitude $\bar{P}_\infty$ was found to be 1.30 ± 0.15. This provides further support for the model for denatured PGK in which the polypeptide chain behaves as a random polymer chain with excluded volume interactions.

3.2.3. High q scattering

For $q \geqslant 1.4b^{-1}$ scattering reflects the local conformation of the chain which roughly behaves as a rigid rod of length b. Furthermore scattering become sensitive to the chemical structure of the chain so that its apparent cross-section has to be taken into account. In this case, a suitable model to describe the neutron scattering spectrum of the chain is the wormlike chain model of Porod and Kratky [44–47] with a finite apparent gyration radius of cross-section, R_c [30]. The reduced structure factor of such a chain can be written [30,48]

$$P_R(q) = \frac{1}{qL}\left(\pi + \frac{4}{3qb}\right)\exp[-(q^2R_c^2/2)]. \qquad (8)$$

According to Ref. [30] this expression is expected to be valid for $1.4b^{-1} \leqslant q \leqslant 1.8R_c^{-1}$, provided that $b > R_c$. For proteins in D_2O the exponential factor of Eq. (8) leads to a decrease of the reduced scattering intensity with q^2. This sharp decrease in the scattering intensity is probably responsible for the absence of a rise in the Kratky plot for denatured PGK (Fig. 3). Unfortunately, the accuracy of the present measurements is not sufficient to allow a meaningful fitting of Eq. (8) to the data in the required q range. Furthermore, the results in the high q range are very sensitive to the background subtraction. However, it is not unreasonable to expect that an improvement in the data quality is feasible and that it will become possible to determine the structural parameters L, b and R_c.

For heteropolymers, such as proteins, the Porod–Kratky description might be reasonable when the solute is in a very good solvent where the effective interactions between different monomers of the chain are repulsive. In this case the values of L, b and R_c should be regarded as averages over the heterogeneities of the chain. When the solvent quality decreases, interactions between some monomers will become attractive whereas most of the others will remain repulsive. Amino acids either far apart or next to each other along the chain can be involved in such attractive interactions. As a result clusters are likely to form. If the local clusters are not too numerous the random polymer description may remain valid. However the apparent contour length L of the chain may shorten whereas its statistical length b and gyration radius of cross-section R_c will increase. In this way the determination of L, b and R_c can yield information about the average residual local structure.

4. Conclusions

The present analysis of the scattering data demonstrates that PGK is highly unfolded in 4 M guanidinium chloride. The radius of gyration changes from 23.4 ± 0.2 Å for the native protein to 71.5 ± 2.0 Å in 4 M GdnDCl. The value of the exponent $\nu = 0.58 \pm 0.02$ is close to the theoretical value of 0.588 given by a model for the denatured protein in which it behaves as a homopolymer in a good solvent, i.e. with excluded volume interactions. This means that all, or almost all, the amino acid residues are solvated at such denaturant concentrations. It may well turn out that the excluded volume chain description of the protein configurational distribution is general for proteins in extreme denaturing conditions [49]. However, some proteins such as bovine pancreatic trypsin inhibitor, ribonuclease A, and thioredoxin [50] may require more stringent denaturing conditions than the one used in the present work to completely lose their secondary structure and behave as excluded volume chains.

Some short sequences of proteins, when taken out of the folded protein, i.e. in the absence of stabilizing tertiary interactions, can still have a tendency to adopt the conformation present in the folded protein [51]. Thus, one would not expect the protein in physiological denatured states to behave as a completely random coil as local sequences of amino acids still manifest conformational preferences. However, the extent that this is still true in highly denaturing solvents remains to be

determined. The question arises as to whether the finding that the excluded volume random coil description fits the present data is consistent with the increasing body of data indicating that proteins possess residual structure in denatured states. The majority of the experiments performed hitherto have been on proteins under mildly denaturing conditions where they are still compact with residual secondary or tertiary structure. Clearly, in these cases the excluded volume random coil description is expected to be inapplicable. Evidence for residual structure also exists in samples of proteins under highly denaturing conditions. The NMR data on 434-repressor in 7 M urea have provided evidence that a cluster of hydrophobic residues exists [21]. However, this cluster concerns residues that are fairly close in the sequence (residues 54 to 59) and occurs in only 20–30% of the configurations. Some clusters such as these might not significantly affect SAS profiles. It is unclear however as to whether the presence of nonlocal interactions would be consistent with the above data. Evidence for the existence of nonlocal interactions in some highly but possibly insufficiently denatured proteins has been provided by fluorescence energy transfer experiments [52]. What is clear is that a complete understanding of the denatured states of proteins will require an accumulation of data on proteins denatured in different and precisely defined ways using many different experimental methods and theoretical approaches.

References

[1] M.E. Goldberg, Trends Biochem. Sci. 10 (1985) 388.
[2] T.E. Creighton, Proteins, structure and molecular properties (W.H. Freeman, New York, 1983).
[3] J.R. Huth, F. Perini, O. Lockridge, E. Bedows and R.W. Ruddon, J. Biol. Chem. 268 (1993) 16472.
[4] O.B. Ptitsyn, J. Protein Chem. 6 (1987) 273.
[5] P.L. Privalov, Ann. Rev. Biophys. Chem. 18 (1989) 47.
[6] C. M. Dobson, Curr. Opin. Struct. Biol. 3 (1993) 57.
[7] T.E. Creighton, Curr. Opin. Struct. Biol. 1 (1991) 5.
[8] D. Shortle, Curr. Opin. Struct. Biol. 3 (1993) 66.
[9] M. Ohgushi and A. Wada, FEBS Letters 164 (1983) 21.
[10] C. Tanford, Adv. Protein Chem. 23 (1968)121.
[11] A. Fersht and L. Serrano, Curr. Opin. Struct. Biol. 3 (1993) 75.
[12] D. Shortle and A.K. Meeker, Proteins 1 (1986) 81.
[13] R.L. Baldwin, Curr. Opin. Struct. Biol. 3 (1993) 84.
[14] S.E. Radford, C.M. Dobson and P.A. Evans, Nature 358 (1992) 302.
[15] E.E. Lattman, Curr. Opin. Struct. Biol. 4 (1994) 87, and references therein.
[16] P. Calmettes, B. Roux, D. Durand, M. Desmadril and J.C. Smith, J. Mol. Biol. 231 (1993) 840.
[17] J.A. Flanagan, M. Kataoka, T. Fujisawa and D.M. Engelman, Biochemistry 32 (1993) 10359.
[18] M. Kataoka, Y. Hagihara, K. Mihara and Y. Goto, J. Mol. Biol. 229 (1993) 591.
[19] T.R. Sosnick and J. Trewhella, Biochemistry 31 (1992) 8329.
[20] G. Damaschun, H. Damaschun, K. Gast, R. Misselwitz, J.J. Müller, W. Pfeil and D. Zirwer, Biochemistry 32 (1993) 7739.
[21] D. Neri, M. Billeter, G. Wider and K. Wuthrich, Science 257 (1992) 1559.
[22] H.C. Watson, N.P.C. Walker, P.J. Shaw, T.N. Bryant, P.L. Wendell, L.A. Fothergill, R.E. Perkins, S.C. Comoy, M.J. Dobson, M.F. Tuite, A.J. Kingsman and S.M. Kingsman, EMBO J. 1 (1982) 1635.
[23] J.P. Yon, M. Desmadril, J.M. Betton, P. Minard, N. Ballery, D. Missiakis, S. Gaillard-Martin, D. Perahia and L. Mouawad, Biochimie 72 (1990) 417.
[24] P.G. de Gennes, Scaling concepts in polymer physics (Cornell Univ. Press, Ithaca, 1979).
[25] J. des Cloizeaux and G. Jannink, Polymers in solution: Their modelling and structure (Clarendon Press, Oxford, 1990).
[26] P. Minard, M. Desmadril, N. Ballery, D. Perahia, L. Hall and J.M. Yon, Eur. J. Biochem. 183 (1989) 419.
[27] T. Bucher, Methods Enzymol. 1 (1955) 415.
[28] P.K. Smith, R.I. Krohm, G.T. Hermanson, A.K. Mallia, F.H. Gatner, M.O. Provenzo, E.K. Fujimoto, H.M. Goebe, B.J. Olson and D.C. Klerc, Anal. Biochem. 150 (1985) 76.
[29] W. Kunz, P. Calmettes and P. Turq, J. Chem. Phys. 92 (1990) 2367.
[30] M. Rawiso, R. Duplessix and C. Picot, Macromolecules 20 (1987) 630.
[31] A. Guinier and G. Fournet, Small angle scattering of X-rays (Wiley, New York, 1955).
[32] A.A. Timchenko and S.N. Tsyuryupa, Biophysics 27 (1982) 1065.
[33] O.B. Ptitsyn, M.Y. Pavlov, M.A. Sinev and A.A. Timchenko, in: Multidomain proteins, eds. L. Patty and P. Friedrich (1986) p. 9.
[34] N. Ballery, P. Minard, M. Desmadril, J.H. Betton, D. Perahia, L. Mouaward, L. Hall and J.M. Yon, Protein Engin. 3 (1990) 199.
[35] P.J. Flory, Principles of polymer chemistry (Cornell Univ. Press, Ithaca, 1953).
[36] J.C. Le Guillou and J. Zinn-Justin, Phys. Rev. Letters 39 (1977) 95.
[37] P. Debye, J. Phys. Colloid Chem. 51 (1947) 18.
[38] T. Ohta, Y. Oono and K.F. Freed, Phys. Rev. A 25 (1982) 2801.
[39] R.G. Kirste and R.C. Oberthur, Small angle X-ray scattering, eds. O. Glatter and O. Kratky (Academic Press, New York, 1982) p. 387.
[40] B.H. Zimm, J. Chem. Phys. 16 (1948) 1093.
[41] T.A. Witten, J. Chem. Phys. 76 (1982) 3300.

[42] J. des Cloizeaux and B. Duplantier, J. Phys. Letters 46 (1982) L457.
[43] I. Noda, M. Imai, T. Kitano and M. Nagasawa, Macromolecules 16 (1983) 425.
[44] G. Porod, Monatsh. Chem. 80 (1949) 251.
[45] O. Kratky and G. Porod, Recl. Trav. Chim. Pays-Bas 68 (1949) 1106.
[46] H.E. Daniels, Proc. Roy. Soc. Edinburgh 63 (1952) 290.
[47] J.J. Hermans and R. Ullman, Physica 18 (1952) 951.
[48] J. des Cloizeaux, Macromolecules 6 (1973) 403.
[49] P. Calmettes, D. Durand, J.C. Smith, M. Desmadril, P. Minard and R. Douillard, J. Phys. IV (France) 3 (1993) C8-253.
[50] K.A. Dill, Biochemistry 29 (1990) 7133.
[51] H. J. Dyson and P. Wright, Curr. Opin. Struct. Biol. 3 (1993) 60.
[52] D.S. Gottfried and E. Haas, Biochemistry 31 (1992) 12353.